

Key Points:

- Ocean internal variability is important when evaluating ocean variables
- Ocean adjustment time scales are faster in the Atlantic than the Pacific due to basin dynamics
- Gridded contours of time scales reflect general ocean circulation patterns

Supporting Information:

- Figure S1

Correspondence to:

E. Hogan,
eehogan2@illinois.edu

Citation:

Hogan, E., & Srivier, R. L. (2019). The effect of internal variability on ocean temperature adjustment in a low-resolution CESM initial condition ensemble. *Journal of Geophysical Research: Oceans*, 124, 1063–1073. <https://doi.org/10.1029/2018JC014535>

Received 3 SEP 2018

Accepted 28 JAN 2019

Accepted article online 30 JAN 2019

Published online 16 FEB 2019

The Effect of Internal Variability on Ocean Temperature Adjustment in a Low-Resolution CESM Initial Condition Ensemble

E. Hogan¹  and R. L. Srivier¹ 

¹Department of Atmospheric Sciences, University of Illinois at Urbana Champaign, Urbana, IL, USA

Abstract Due to its large heat capacity and circulation, the ocean contributes significantly to global heat uptake, global heat transport, spatial temperature patterns, and variability. Quantifying ocean heat uptake across different temporal and spatial scales is important to quantify Earth's climate response to anthropogenic warming. Here we evaluate ocean adjustment time scales from two different fully coupled climate model ensembles using the Community Earth System Model. Both ensembles use the same model version, anthropogenic and natural forcings, and coupling configurations, but we initialize the ensembles in two different ways: (1) sampling joint internal variability of the ocean–atmosphere system (unique atmosphere and ocean conditions) and (2) sampling the internal variability of the atmosphere only (unique atmosphere, identical ocean conditions). Uncertainty due to internal variability is used as a proxy to quantify the time scales of ocean temperature adjustment at different depths and basins in Community Earth System Model. Time scales of equilibration are longer in the deep ocean than the upper ocean, highlighting the vertical structure of dynamic adjustment. The Atlantic equilibrates on shorter time scales (82 years above 1,000 m, 140 years below 1,000 m) relative to the Pacific (106 years above 1,000 m, 444 years below 1,000 m) in Community Earth System Model due to the large North Atlantic Deep Water formation and strong overturning circulation in the Atlantic. These results have broad implications for analyzing internal climate variability, ocean adjustment, and drift in global coupled model experiments and intercomparisons.

Plain Language Summary The ocean is an important component of the Earth's climate, and monitoring heat uptake into the ocean is important for assessing climate change. Here we use two climate model ensembles created using the same Earth System model (Community Earth System Model) that were initialized differently. The difference between the two models shows uncertainty due to the internal variability of the ocean. We find the deep ocean takes longer to adjust than the upper ocean. The Atlantic has faster adjustment time scales (82 years above 1,000 m, 140 years below 1,000 m) compared to the Pacific (106 years above 1,000 m, 444 years below 1,000 m) in the Community Earth System Model. These results have broad implications for studying climate change and internal climate variability in Earth system models.

1. Introduction

The global ocean is an important component of the climate system due to its ability to take up excess heat in the Earth's system. The waters of the ocean cover approximately 70% of our planet's surface, and consequently, the interaction of the ocean with the atmosphere occurs across vast spatial scales. Since 1950, the ocean has absorbed 80 to 90% of the Earth's radiation imbalance due to anthropogenic forcing (Intergovernmental Panel on Climate Change, 2014; Levitus et al., 2000, 2005; Marshall & Zanna, 2014). This uptake has influenced the rate and surface pattern of atmospheric warming but also has important implications for the distribution of heat within the ocean (Garuba & Klinger, 2016) and sea level rise trends (Hogan & Srivier, 2017; Kuhlbrodt & Gregory, 2012), as thermal expansion is a proxy for temperature changes in the ocean. The ocean is able to affect climate through its high heat capacity relative to the surrounding land (Clark et al., 2002). Because of this high heat capacity, temperature variability is less and signal-to-noise ratios are larger in the ocean compared to the atmosphere. Thus, ocean heat uptake and sea level rise provide strong evidence of trends in planetary warming on interannual to interdecadal time scales (Cheng et al., 2017). Better understanding of ocean variability and internal variations on different spatial scales provides continued information about how the Earth continues to respond to a changing climate.

Along with its large heat capacity, the ocean affects climate through its ability to transport heat across different latitudes, longitudes, and vertical depths (Garuba & Klinger, 2016; Yang & Zhu, 2011). This causes considerable differences in density patterns across the two main ocean basins (Atlantic and Pacific). Meridional cross sections displaying observed temperature, salinity, and density for the Atlantic and Pacific are shown in Figure 1 (Locarnini et al., 2013; Zweng et al., 2013). Ocean density is a function of ocean temperature, salinity, and pressure (McDougall et al., 2003). Warm, salty surface waters in the Atlantic are transported north, where cooling leads to sinking at high latitudes. This process is an important component of the Atlantic Meridional Overturning Circulation (Weaver et al., 1999). Atlantic Meridional Overturning Circulation is responsible for 25% of the total northward transport of heat by the atmosphere and ocean (Hall & Bryden, 1982; Trenberth & Caron, 2001). Deep water formation does not occur in the North Pacific, as although the surface waters are cold, they are not dense enough to sink more than a few hundred meters (Broecker, 1991; Weaver et al., 1999). Additionally, the Atlantic extends further north than the Pacific (Figure 1; Warren, 1983). The surface waters of the North Pacific are thought to be less saline for several reasons. There is nearly double the evaporation over the North Atlantic than the North Pacific (Baumgartner & Reichel, 1975; Warren, 1983), related to the warmer sea surface temperatures in the Atlantic Northern basin, partially due to the presence of the Gulf Stream. Additionally, the narrower shape of the Atlantic basin is thought to be favorable for sinking, which contrasts with the wider Pacific (Cai, 2006; Jones & Cessi, 2017). In the magnitudes of observed density between the Atlantic and Pacific (Figures 1e and 1f), density is higher in the North Atlantic than at similar latitudes in the Pacific, where less dense water is closer to the surface. The contrasting higher density surface waters in the North Atlantic (Figure 1, panel e) cause instability and sinking. The Atlantic Meridional Overturning Circulation leads to upwelling of cooler water at lower latitudes. This poleward movement of surface water and sinking at high latitudes is a primary method through which the global ocean takes up heat. Here we evaluate uncertainty in model projections of these dynamics, important in the evaluation of how ocean variability influences heat uptake and storage and in understanding interpretations about climate change.

Ocean heat uptake is a key area of interest for climate scientists. Research in this area has greatly improved in recent decades as increased temporal and spatial observations from Argo profiling floats (Gould et al., 2004; Rommich and Owens, 2000) and satellite observations (Leuilette et al., 2004) have led to more complete observational coverage of the global ocean. Ocean heat uptake was a critical process in explaining temperature changes during the climate hiatus (1998–2012), when surface atmospheric temperature showed very small increases, or potentially even a slight negative trend (Easterling & Wehner, 2009; Foster & Rahmstorf, 2011; Frankcombe et al., 2015; Meehl et al., 2011) compared to previous decades. However, while there was a hiatus in atmospheric temperature, there was a continued net energy flux into the climate system (Hansen et al., 2006; Trenberth et al., 2009), meaning this energy was being stored elsewhere (Trenberth et al., 2009; Trenberth & Fasullo, 2010).

Climate models are often evaluated to provide information on changes in the deep ocean, and studies have found that ocean heat uptake contributes considerably to climate model spread (Bóe et al., 2009). Here we focus on quantifying the time scales of adjustment in the ocean using fully coupled, comprehensive model ensemble runs simulated by the Community Earth System Model (CESM; Sriver et al., 2015; Hogan & Sriver, 2017; Vega-Westhoff & Sriver, 2017; Haugen et al., 2018; -- <https://journals.ametsoc.org/doi/abs/10.1175/JCLI-D-17-0782.1>). We evaluate ocean internal variability in temperature as a proxy for ocean adjustment and assess this variability on both global- and basin-scale spatial regions, and throughout different ocean depths.

2. Materials and Methods

We present results from two climate change ensemble experiments using the low-resolution version of CESM (Shields et al., 2012), introduced by Sriver et al. (2015), Hogan and Sriver (2017), and Vega-Westhoff and Sriver (2017). Each ensemble uses the same preindustrial control simulation with constant preindustrial radiative forcing, which was spun up with a full-coupled atmosphere–ocean component, until the deep ocean had reached approximate dynamic equilibrium (by year 4200). This method reduces the effect of model ocean drift from affecting our estimates of ocean variables including the deep ocean (Hogan & Sriver, 2017).

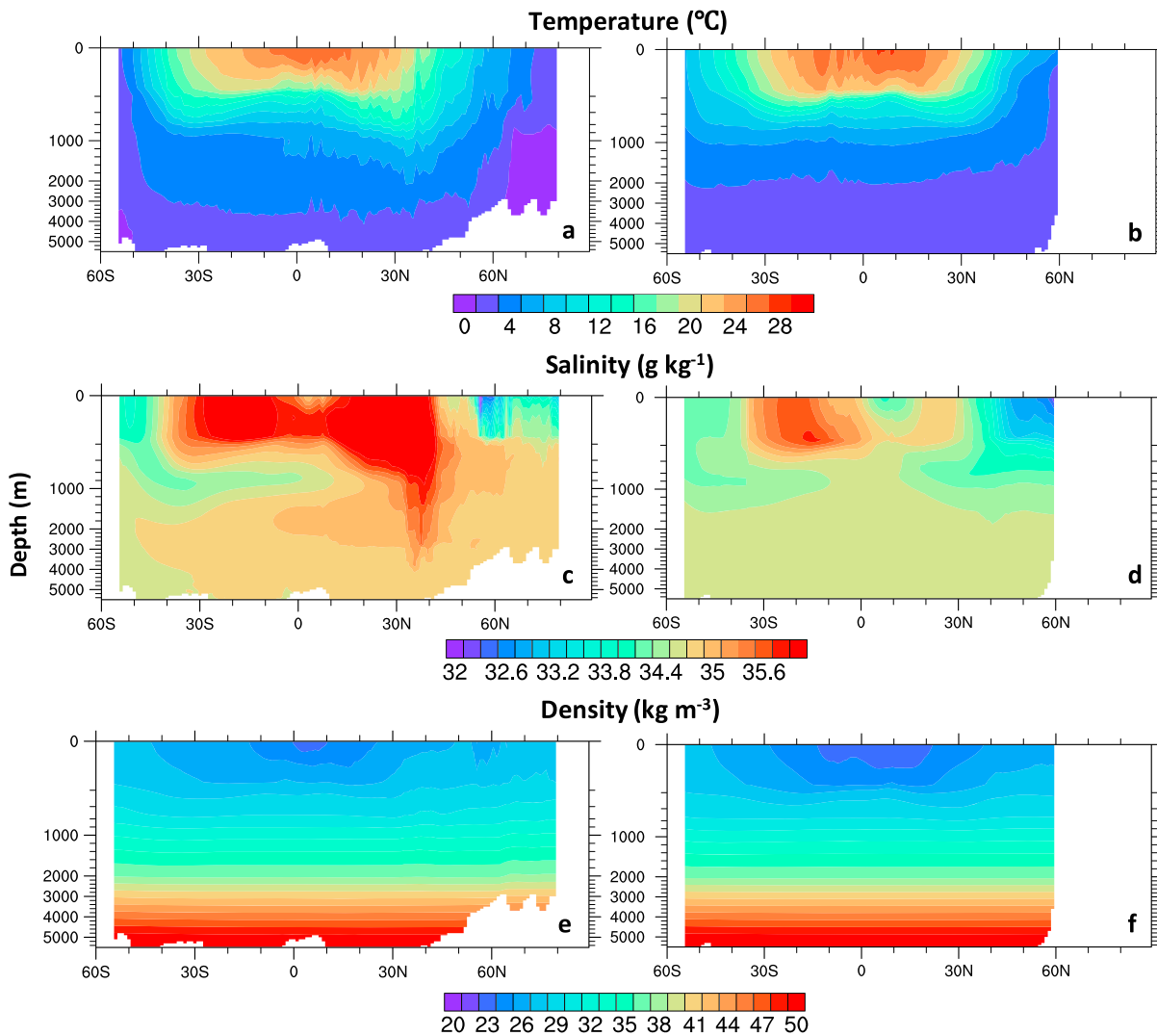


Figure 1. Observed annual climatology cross sections of (a, c, and e) Atlantic and (b, d, and f) Pacific ocean temperature (a and b), salinity (c and d), and density (e and f). Observations span from 1955 to 2012. Data sourced from National Centers for Environmental Information (Locarnini et al., 2013; Zweng et al., 2013).

The first of the two CESM ensembles used in this study (CESM-AO) is composed of 50 ensemble members. We initialized historical simulations starting in 1850 from instantaneous snapshots of the fully coupled model state (with unique atmosphere, ocean, land, and sea ice conditions for each ensemble member). Ensemble runs were branched every 100 years from the control simulation starting at year 4200 in the fully coupled preindustrial control simulation. Each historical simulation was run out to 2,100 using Representative Concentration Pathway (RCP) 8.5, the “business-as-usual” idealized forcing scenario (Moss et al., 2010). Hogan and Srivier (2017) provide more details on the low-resolution version of CESM, with details on biases, and the computational trade-off required to eliminate drift by spinning up the control for 4,200 years.

We additionally performed a second CESM ensemble experiment (CESM-A), where the initialization method used was similar to the Large Ensemble Experiment (LENS; Kay et al., 2015). In LENS, transient runs were initialized by perturbing atmospheric temperature at the “round-off level,” or 14th decimal place at every grid point, while keeping the initial conditions for the other model components (e.g., the ocean) identical between each simulation. As the ocean is identical between each model run, the LENS-style ensembles sample only the internal variability of the atmosphere. We used this method to initialize runs corresponding to year 7,000 of our preindustrial control run simulation. We conducted a 40-member ensemble

using ocean, land, and sea ice conditions from year 7000 and sampling atmospheric internal variability only using the LENS round-off method (CESM-A). Due to computational constraints, simulations in CESM-A are performed for the historical period only (1850–2005). In the present study, we use the historical period in all analysis and ensemble comparisons.

Differences between variability in the ocean between these two CESM ensembles are evaluated in Hogan and Srivier (2017) and are briefly highlighted here. As the atmosphere equilibrates on time scales of approximately weeks to months, we see very similar ranges of global atmospheric temperature variability between CESM-AO and CESM-A. However, due to the large thermal inertia and long time scales of temperature adjustment in the ocean, there is a discrepancy in the spread of global ocean temperature between the two ensembles. Global ocean temperature variability in CESM-A begins at 0, as each simulation in this ensemble is branched from an identical ocean state. By the end of the 155 years (1850–2005), global ocean variability in CESM-A has increased, but is only a fraction of the total variability seen in CESM-AO. This demonstrates the longer adjustment time scale of the ocean compared to the atmosphere, and emphasizes the importance of sampling ocean internal variability when analyzing coupled climate oscillations and variability.

3. Results

We evaluate changes in temperature variability with time in the global ocean as a function of depth (Figure 2), with colors presenting the 95% range in ensemble spread (difference between the 0.025 and 0.975 quantiles). We evaluate this percentage range in order to effectively compare temperature variability in two ensembles that have a different number of simulations (CESM-AO has 50, CESM-A has 40). Figures 2a and 2b examine the change in spread of global temperature in the model ensembles with vertical depth from 1850 to 2005. Here we see considerably more variability in the upper ocean (surface to 1,000 m) in both ensembles when compared to the deep ocean, where the magnitude of variability remains close to zero. The deep ocean equilibrates on considerably longer time scales, and at these depths we show a low magnitude of variability, whereas upper ocean mixing enhances ensemble spread above 1,000 m. In order to compare differences between the two ensembles, we show the spread of CESM-AO minus the spread of CESM-A (Figure 2c), where red contours depict a larger 95% spread in variability in CESM-AO and blue contours depict larger 95% spread in variability in CESM-A. Note the change to a linear scale of the y axis in Figure 2c, chosen to focus on the deep ocean.

We see considerably increased variability in CESM-AO compared to CESM-A throughout the middle and deep ocean (below 1,000 m). The CESM-A ensemble does not sample internal ocean variability and thus underestimates the deep ocean variability compared to CESM-AO. However, throughout time, we see the increased magnitude of variability in CESM-AO diminishing. Ocean variability in CESM-A increases with time, as the initialization perturbation from the atmosphere is transmitted throughout the ocean, consistent with results found by Hogan and Srivier (2017).

We evaluate temperature spread differences shown in Figure 2 for two ocean depths (Figure 3). We consider the upper ocean (0–1,000 m) to isolate the subsurface mixed layer, where temperature variability is larger. In addition, we consider the deeper ocean layer (1,000–5,000 m), where temperature variability is lower, vertical grid spacing is larger, and differences between CESM-AO and CESM-A are also larger. We see variability in the upper ocean reaching a similar magnitude by the end of the simulations (2005) between CESM-AO and CESM-A, emphasizing the shorter time scales on which the upper ocean adjusts dynamically to a surface temperature perturbation. In contrast, below 1,000 m, we see that the magnitude of the range of variability in CESM-A reaches only a fraction of CESM-AO, even by the end of the simulations in 2005. Additionally, at the beginning of the simulations, variability is close to 0 in CESM-A. This result is expected as each model simulation is branched from an identical ocean state. With time, ocean temperature adjusts slowly and variability increases in CESM-A. However, the full range of global temperature variability seen in CESM-AO will not be reached by CESM-A until 2120 (not shown; this value was found using the same method used for values calculated in Table 1).

We evaluate ocean temperature variability averaged over the depths described above, and we focus on the two main ocean basins in our model, the Atlantic Ocean and the Pacific Ocean, in order to examine regional differences in the model response and connections to large-scale ocean dynamics (Figure 4). Time scales of

95% Range of Ensemble Variability in Global Ocean Temperature

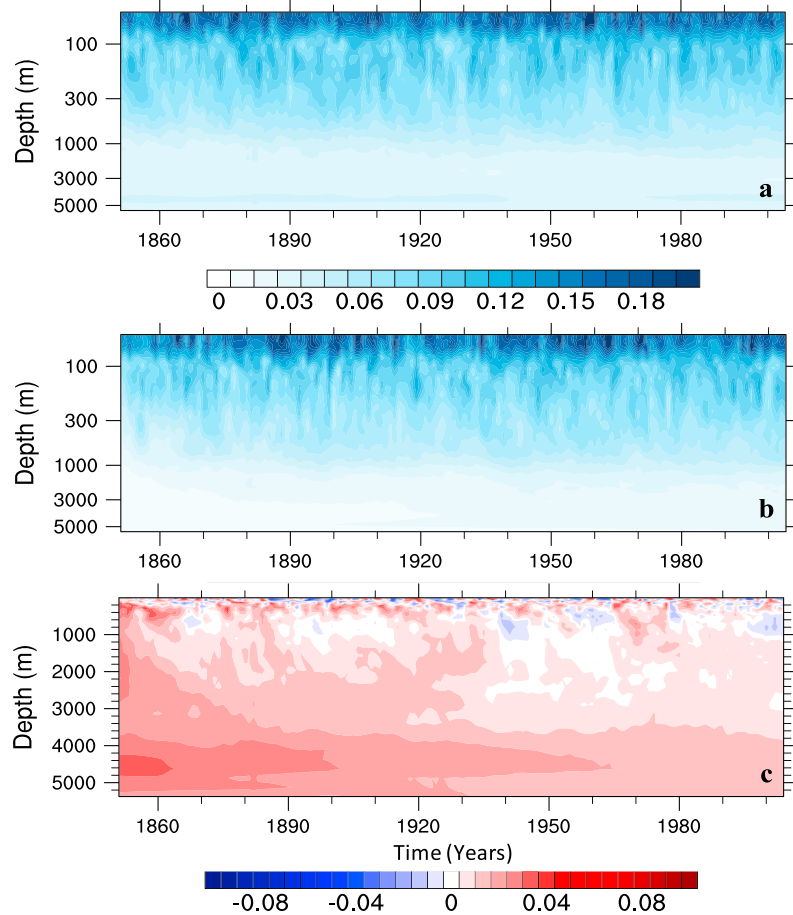


Figure 2. Changes in 95% range of ensemble spread in globally averaged vertical ocean temperature with time. (a) CSM-AO. (b) CSM-A. (c) CSM-AO minus CSM-A. Figures 2a and 2b have a logarithmic y axis and Figure 2c has a linear y axis.

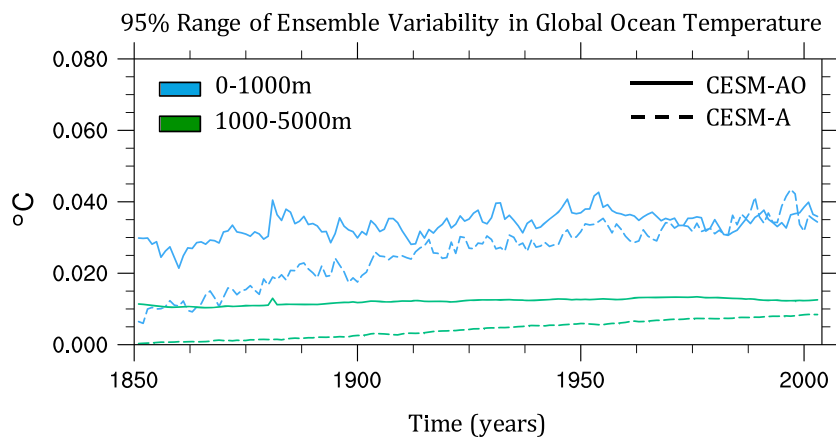


Figure 3. Time series of globally averaged 95% range in ocean temperature across each ensemble, separated into two averaged depths, 0–1,000 m in blue and 1,000–5,000 m in green. CSM-AO is shown in solid lines and CSM-A in dashed lines.

Table 1
Table Displaying the Time Taken (in Years Since 1850) for Model Ocean Temperature in CESM-A to Adjust to the Magnitudes of CESM-AO (Year When Difference in Ensemble Spread = 0 °C)

	Atlantic	Pacific
0–1000 m	82.2 (0.51)	105.8 (0.31)
1000–5000 m	140.3 (0.98)	443.7 (0.86)

Parentheses contain the correlation coefficient of the data to the linear trends used.

ocean circulation between basins are dependent on ocean overturning, deep water formation, and ocean dynamics. The meridional circulation in the Atlantic is faster in general due in part to the production of North Atlantic Deep Water, which does not occur in the North Pacific due to relatively fresher surface water, and thus, the advective time scale is slower (see Figure 1). To quantify the regional differences in ocean temperature adjustment time scales, we averaged over model grid cells corresponding to the Pacific and Atlantic Oceans, ending at 55°S so as to exclude the Southern Ocean. We show the difference in 95% range of variability across both ensembles in the Atlantic (Figure 4a) and the

Pacific (Figure 4b), where red (blue) contours depict a larger (smaller) 95% ensemble spread in CESM-AO compared to CESM-A.

Both basins show the 95% ensemble spread to be larger in CESM-AO, but the differences between temperature variability in the two basins are notable. The Atlantic shows larger differences in spread between

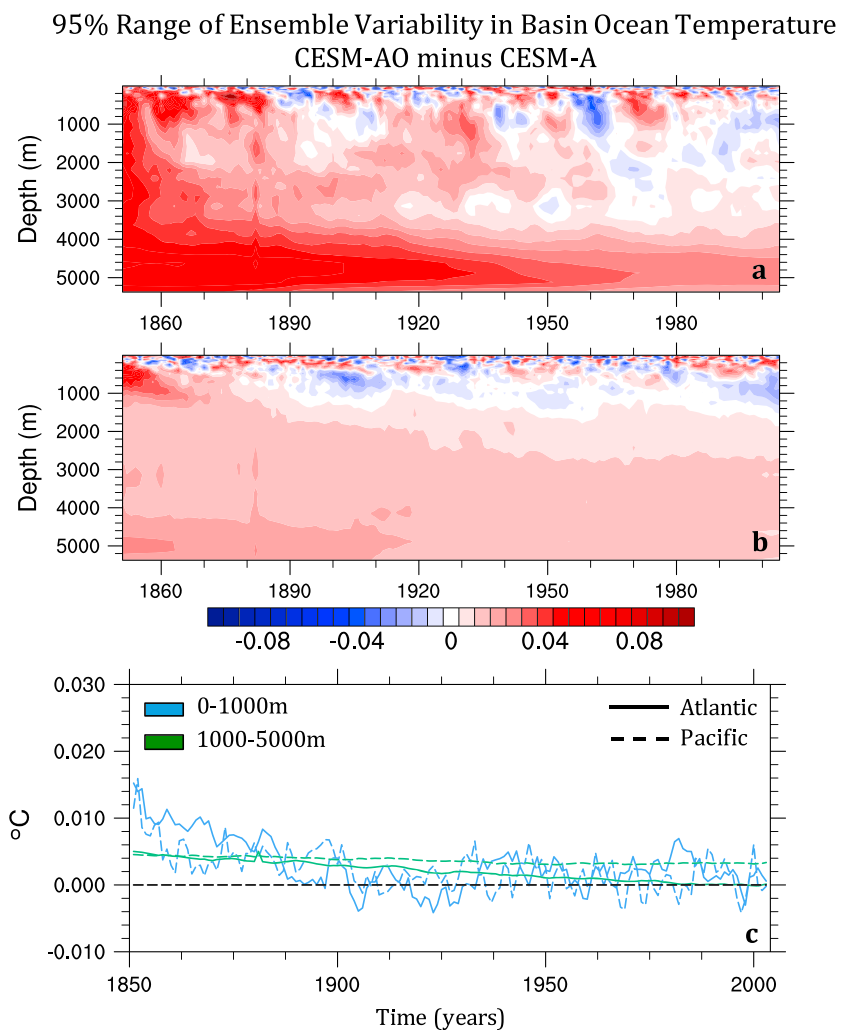


Figure 4. Changes in 95% range of ensemble spread basin averaged vertical ocean temperature with time. (a) CESMAO minus CESM-A in the Atlantic. (b) CESM-AO minus CESM-A in the Pacific. (c) Corresponding time series of the differences in ensemble spread averaged over different depths, 0–1,000 m in blue and 1,000–5,000 m in green. Changes in the Atlantic are displayed in solid lines, and changes in the Pacific are displayed in dashed lines. When the lines are above the dashed black line denoting 0, CESM-AO has greater spread than CESMA for that basin and depth. When the lines are below the dashed black line denoting 0, CESM-A has greater spread than CESM-AO for that basin and depth.

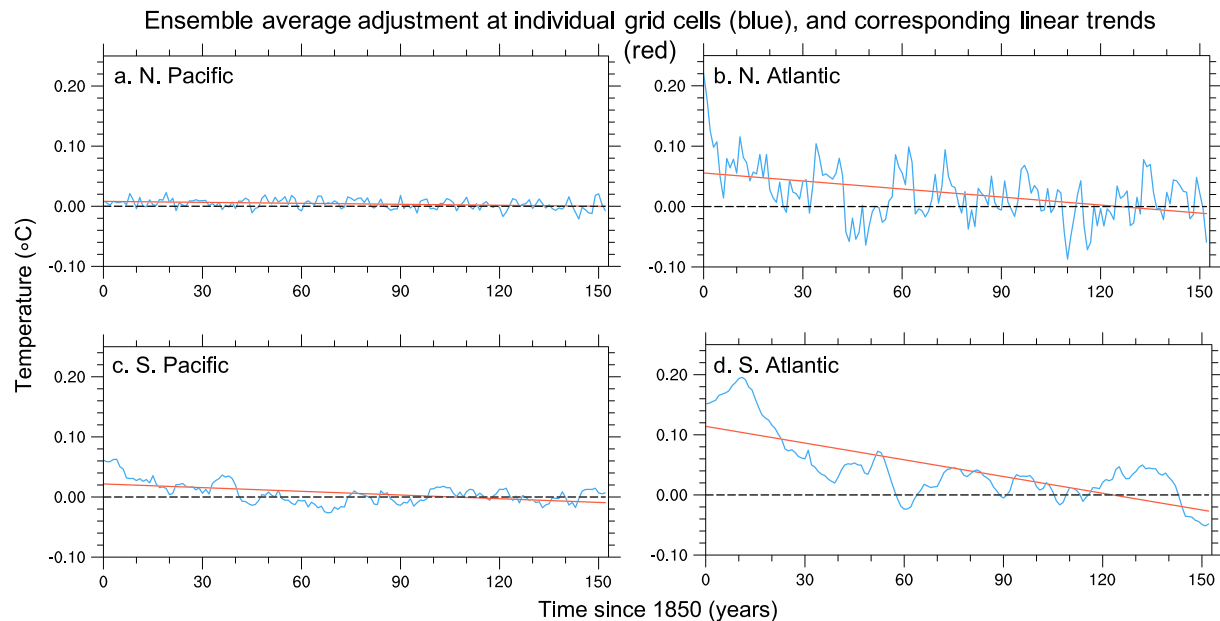


Figure 5. Ensemble average adjustment of CESM-AO minus CESM-A at 2,000 m at individual grid cells (blue) and calculated linear trends (red). North Pacific (55.5°N, 180.5°W), South Pacific (60.5°S, 180.5°W), North Atlantic (55.5°N, 330.5°W), and South Atlantic (60.5°S, 330°W).

ensembles, and these differences reduce quickly; by 1920, differences in spread are similar from the surface down to 3,500 m. In contrast, differences in variability in the Pacific are much less initially, but temperature adjustment in this basin is much slower, shown by similarities in spread by 1920 only reaching approximately down to 1,000 m. In the deep ocean, differences between variability change relatively slowly due to the long time scale of ocean temperature adjustment in this basin. Differences between depths and basins are shown in the time series (Figure 4c) where lines are the difference between 95% variability in CESM-AO and CESM-A, averaged over displayed depths and regions. For each line, we consider the variability between CESM-AO and CESM-A to be equal when the lines reach 0 °C. We provide additional time series of regional effects between North and South Atlantic and Pacific Basins in Figure S1 in the supporting information. In addition to large interbasin variability, we find considerable differences in the trend and variability North and South Atlantic deep ocean temperature adjustment. In addition, the South Pacific equilibrates much faster than the northern counterpart.

We quantify the time scales of ocean adjustment (Table 1) by estimating linear functions for each of our difference lines in Figure 4c and calculating when the fit crosses 0 °C. For the time series showing 95% range above 1,000 m, we estimated a linear trend using the first 100 years of data, and we estimate a linear trend over the range below 1,000 m using the full 155 years. When the difference lines reach 0 °C, the 95% spread in CESM-AO is equal to the 95% spread in CESM-A and we can approximate that the CESM-A ocean has reached equilibrium.

As a test of the linear assumption, we highlight time series of ensemble deep ocean temperature adjustment for four different locations (Figure 5) in the North/South Atlantic and Pacific Basins. We assume a linear temperature adjustment in this paper as a conservative estimate, given the large spatial differences (both horizontally and vertically) in long-term temperature trends and year-to-year temperature variability.

Using our approximated linear trends, we find the ocean to reach 0 °C faster in the upper Atlantic than in the upper Pacific (82.2 years in the Atlantic versus 105.8 in the Pacific), as deep water formation dynamics in the Atlantic enhances ocean mixing, allowing for a faster increase in the spread of variability in CESM-A and therefore a shorter time scale of ocean memory in this basin. The upper ocean also reaches 0 °C faster than below 1,000 m in both ocean basins (58 years faster in the Atlantic and 338 years faster in the Pacific). Here the time scales of ocean memory are enhanced in the deep ocean for both basins, where the effect of ocean mixing is limited, and memory is longer.

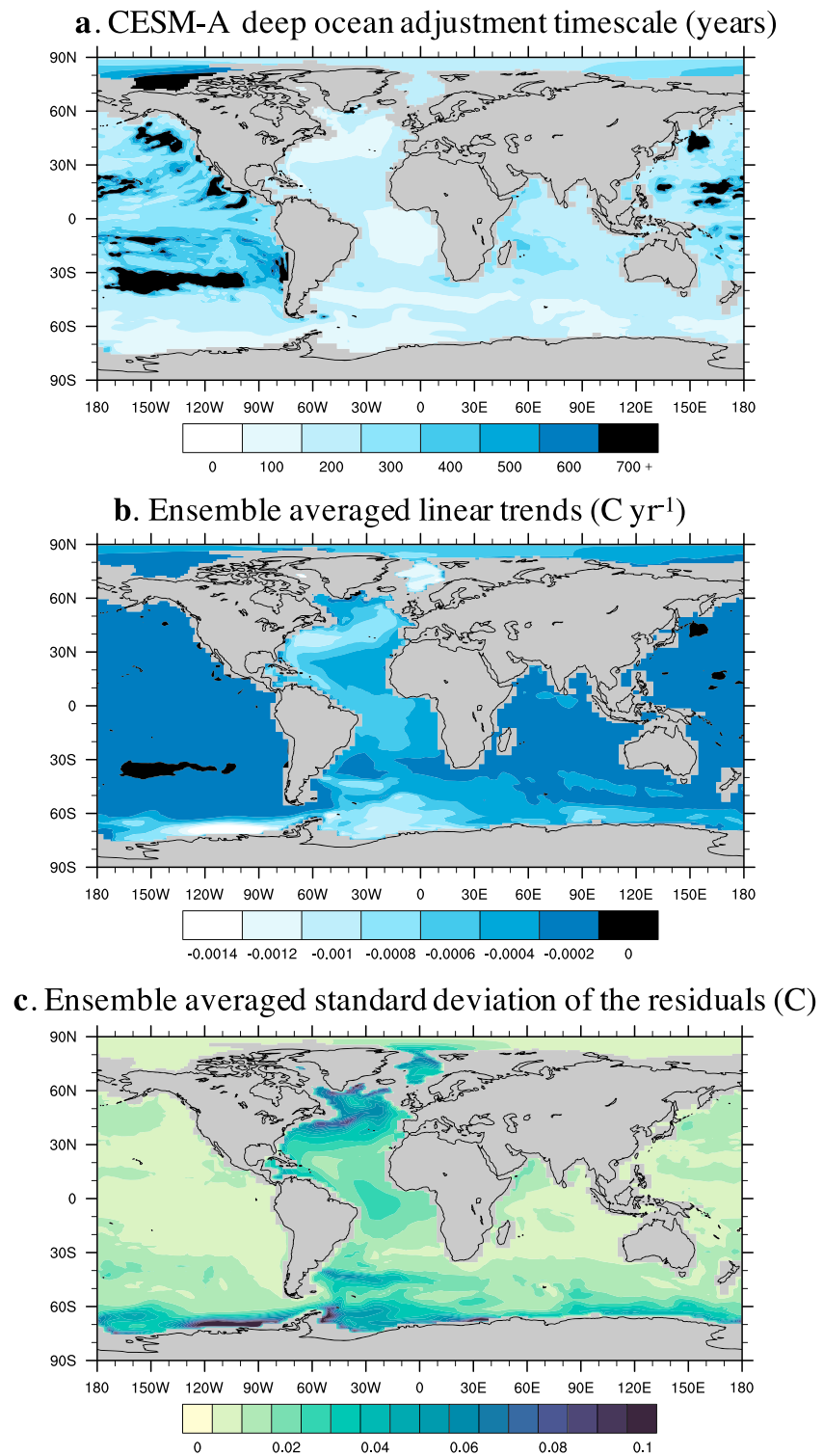


Figure 6. (a) Time taken (years) since 1850 for trends in ocean temperature at 2,000 m over 95% of CESM-A ensemble spread to equal trends in ocean temperature calculated over 95% of CESM-AO ensemble spread. (b) Ensemble averaged linear trends used to calculate times in (a). (c) Ensemble averaged standard deviation of the residuals (linear trend minus the difference between CESM-AO and CESM-A).

We performed some simple uncertainty testing to determine how well our data matches the estimated linear trends we calculated to determine the time taken (Table 1, parentheses). The trends in the deep ocean are approximately linear and our data match the approximate trends with high correlation values. We also have stronger linear correlation in the Atlantic, where adjustment speeds are higher. There is more uncertainty in the upper ocean however, where interannual variability is higher.

We take this analysis a step further by evaluating the time taken for each ocean grid point in CESM-A at 2,000-m depth to equilibrate (Figure 6a). The 2000-m depth was chosen in accordance with other studies examining deep ocean responses to surface forcing (Wunch and Heimbach, 2008). Here at each grid point, we calculated the time taken since the start of our simulations (1850) for the 95% CESM-A ensemble spread in ocean temperature to equal the 95% CESM-AO ensemble spread in ocean temperature. This was done by calculating a linear trend over all 155 years of data for both ensembles at each grid point and finding at which year 95% of the spread became equal. Trend estimates and standard deviations of the residuals for each grid point are shown in Figures 6b and 6c. Grid points contoured in black show regions where the linear trends calculated for CESM-AO and CESM-A produced such a similar gradient, calculated time taken produced unphysical values. These areas are labeled as greater than 700, although we stress that with the extension of our CESM-A simulations out to 2,100, a more definite linear trend may be calculated and these values may be identified with greater accuracy.

We see patterns in Figure 6 mirroring our preliminary basin analysis shown in Figure 4. Times taken for equilibrium in the Atlantic at this depth are much shorter than in the Indian and Pacific Oceans. Deep water formation in the North Atlantic allows for faster water transport and causes these ocean grid points in CESM-A to equilibrate faster than other areas. Differences are also due to large spatial differences in long-term temperature trends and year-to-year temperature variability, which is much larger in the Atlantic Basin (Figures 6b and 6c). Areas in the Pacific show a contrasting longer time taken to reach equilibrium, as the ocean circulation is slower, and it takes longer for this basin to adjust to a temperature perturbation at the surface.

Large swaths of areas situated within the Pacific gyres show contours depicting times longer than 700 years for temperature adjustment. In these areas, trends calculated in CESM-A over the 155-year period are very similar to trends calculated in CESM-AO; that is, ocean variability in CESM-A is increasing very slowly.

4. Conclusions

In this study we evaluate and quantify the time scales of ocean temperature adjustment, in particular focusing on interannual variability in CESM, using two uniquely initialized model ensembles and evaluate how the spread in ocean internal variability changes with time according to depth and ocean basin. The difference between the two CESM ensembles is the presence of ocean internal variability in CESM-AO, while CESM-A samples initial conditions from an identical ocean state, therefore not sampling the internal variability of the ocean. We highlight the time scale of ocean adjustment on a global scale at different depths in the CESM ensembles. We see larger variability in the deep ocean (below 1,000 m) in CESM-AO at all time steps in both basins, although above 1,000-m subsurface ocean mixing allows for shorter ocean memory. We also isolate the effect of internal ocean variability on the spread of temperature between the two largest ocean basins. We find regional differences between the Atlantic and the Pacific, demonstrating the importance of interbasin ocean dynamics on the time scales of ocean memory in this model.

Results have considerable implications for the understanding the importance of ocean memory in both the low-resolution CESM, and in global coupled climate models in general. They reflect the depth dependence of ocean adjustment time scales in coupled global models, which need to be taken into account when considering time variations of deep ocean variability, such as changes in the Atlantic Meridional Overturning Circulation, water mass formation rates such as NADW, and ocean heat uptake. Additionally, results emphasize the implications of the choice of climate model initialization method. The 95% variability of ocean temperature in CESM-A is a fraction of that from CESM-AO for the global ocean, but also on basin scales and particularly in the deep ocean. Variability is similar in the upper ocean (above 1,000 m; Figure 3), and so internal variability throughout the subsurface ocean in CESM-A is faster to reach the full extent of variability seen in CESM-AO. Results also point to the importance of accounting for deep ocean drift, as modeling communities involved in CMIP5 and the upcoming CMIP6 ensemble lack the

computational power required to fully equilibrate their preindustrial control simulations as done here for CESM-AO and CESM-A. Trends due to drift added to ocean variables such as sea level rise can mask the true effect of anthropogenic forcing and can affect interpretations about climate change. Finally, these results reiterate the importance of ocean internal variability and a coupled ocean–atmosphere model control setup when analyzing variability in ocean variables, particularly at depth, where the time scales of ocean memory are longer and internal variability is not well represented. However, results suggest that using a method of initialization such as CESM-A to sample atmospheric variability and surface ocean variability may be sufficient due to the shorter time scales on which these model components equilibrate.

Acknowledgments

The authors declare no conflicts of interest. This study was partially supported by the DOE Program on Coupled Human Earth Systems (PCHES) under DOE Cooperative Agreement DE-SC0016162. Any opinions, findings, and conclusions or recommendations expressed in this material are those of the authors and do not necessarily reflect the views of the funding entities. All data are posted on our departmental server at the University of Illinois: http://manabe.atmos.uiuc.edu/~rsriver/hogan_sriver_2019_jgr_data/.

References

- Baumgartner, A., & Reichel, E. (1975). *The World Water Balance* (p. 179). Amsterdam/Lausanne/NY: Elsevier.
- Böe, J., Hall, A., & Qu, X. (2009). Deep ocean heat uptake as a major source of spread in transient climate change simulations. *Geophysical Research Letters*, *36*, L22701. <https://doi.org/10.1029/2009GL040845>
- Broecker, W. S. (1991). The great ocean conveyor. *Oceanography*, *4*(2), 79–89. <https://doi.org/10.5670/oceanog.1991.07>
- Cai, W. (2006). Zonal extent of oceans, high latitude fresh water supplies and the thermohaline circulation. *Quarterly Journal of the Royal Meteorological Society*, *124*(547), 811–828. <https://doi.org/10.1002/qj.49712454708>
- Cheng, L., Trenberth, K. E., Fasullo, J., Abraham, J., Boyer, T. P., von Schuckmann, K., & Zhu, J. (2017). Taking the pulse of the planet. *Eos*, *98*. <https://doi.org/10.1029/2017EO081839>
- Clark, P. U., Pisias, N. G., Stocker, T. F., & Weaver, A. J. (2002). The role of the thermohaline circulation in abrupt climate change. *Nature*, *415*(6874), 863–869. <https://doi.org/10.1038/415863a>
- Easterling, D. R., & Wehner, M. F. (2009). Is the climate warming or cooling? *Geophysical Research Letters*, *36*, L08706. <https://doi.org/10.1175/JCLI-D-17-0011.1>
- Foster, G., & Rahmstorf, S. (2011). Global temperature evolution 1979–2010. *Environmental Research Letters*, *6*(4). <https://doi.org/10.1088/1748-9326/6/4/044022>
- Frankcombe, L. M., England, M. H., Mann, M. E., & Steinmann, B. A. (2015). Separating internal variability from the externally forced climate response. *Journal of Climate*, *28*(20), 8184–8202. <https://doi.org/10.1175/JCLI-D-15-0069.1>
- Garuba, O. A., & Klinger, B. A. (2016). Ocean heat uptake and interbasin transport of the passive and redistributive components of surface heating. *Journal of Climate*, *29*(20), 7507–7527. <https://doi.org/10.1175/JCLI-D-16-0138.1>
- Gould, J., Roemmich, D., Wijffels, S., Freeland, H., Ignaszewsky, M., Pouliquen, S., et al. (2004). Argo profiling floats bring new era of in situ ocean observations. *Eos, Transactions of the American Geophysical Union*, *85*, 185–191. <https://doi.org/10.1029/2004EO190002>
- Hall, M. M., & Bryden, H. L. (1982). Direct estimates and mechanisms of ocean heat transport. *Deep-Sea Research*, *29*(3), 339–359. [https://doi.org/10.1016/0198-0149\(82\)90099-1](https://doi.org/10.1016/0198-0149(82)90099-1)
- Hansen, J., Sato, M., Ruedy, R., Lo, K., Lea, D. W., & Medina-Elizade, M. (2006). Global temperature change. *Proceedings of the National Academy of Sciences of the United States of America*, *103*(39), 14,288–14,293. <https://doi.org/10.1073/pnas.0606291103>
- Haugen, M. A., Stein, M. L., & Moyer, E. J. (2018). Estimating Changes in Temperature Distributions in a Large Ensemble of Climate Simulations Using Quantile Regression. <https://journals.ametsoc.org/doi/abs/10.1175/JCLI-D-17-0782.1>
- Hogan, E., & Srivier, R. L. (2017). Analyzing the effect of ocean internal variability on depth-integrated steric sea-level rise trends using a low-resolution CESM ensemble. *WATER*, *9*(7), 483. <https://doi.org/10.3390/w9070483>
- Intergovernmental Panel on Climate Change (2014). Observations: Ocean Pages. In *Climate Change 2013 – The Physical Science Basis: Working Group I Contribution to the Fifth Assessment Report of the Intergovernmental Panel on Climate Change* (pp. 255–316). Cambridge: Cambridge University Press. <https://doi.org/10.1017/CBO9781107415324.010>
- Jones, C. S., & Cessi, P. (2017). Size matters: Another reason why the Atlantic is saltier than the Pacific. *Journal of Physical Oceanography*, *47*, 2,843–2,859. <https://doi.org/10.1175/JPO-D-17-0075.1>
- Kay, J., Deser, C., Phillips, A., Mai, A., Hannay, C., Strand, G., et al. (2015). The Community Earth System Model (CESM) large ensemble project: A community resource for studying climate change in the presence of internal climate variability. *Bulletin of the American Meteorological Society*, *96*(8), 1333–1349. <https://doi.org/10.1175/BAMS-D-13-00255.1>
- Kuhlbrodt, T., & Gregory, J. M. (2012). Ocean heat uptake and its consequences for the magnitude of sea level rise and climate change. *Geophysical Research Letters*, *39*, L18608. <https://doi.org/10.1029/2012GL052952>
- Leuliette, E. W., Nerem, R. S., & Mitchum, G. T. (2004). Calibration of TOPEX/Poseidon and Jason altimeter data to construct a continuous record of mean sea level change. *Marine Geodesy*, *27*(1-2), 79–94. <https://doi.org/10.1080/01490410490465193>
- Levitus, S., Antonov, J. I., & Boyer, T. P. (2005). Warming of the world ocean, 1955–2003. *Geophysical Research Letters*, *32*, L02604. <https://doi.org/10.1029/2004GL021592>
- Levitus, S., Antonov, J. I., Boyer, T. P., & Stephens, C. (2000). Warming of the world ocean. *Science*, *287*(5461), 2225–2229. <https://doi.org/10.1126/science.287.5461.2225>
- Locarnini, R. A., Mishonov, A. V., Antonov, J. I., Boyer, T. P., Garcia, H. E., Baranova, O. K., et al. (2013). World ocean atlas 2013, Volume 1. In S. Levitus & A. Mishonov (Eds.), *Temperature* (Vol. 73, p. 40). NOAA atlas NESDIS.
- Marshall, D. P., & Zanna, L. (2014). A conceptual model of ocean heat uptake under climate change. *Journal of Climate*, *27*(22), 8444–8465. <https://doi.org/10.1175/JCLI-D-13-00344.1>
- McDougall, T. J., Jackett, D. R., Wright, D. G., & Feistel, R. (2003). Accurate and computationally efficient algorithms for potential temperature and density of sea water. *Journal of Atmospheric and Oceanic Technology*, *20*(5), 730–741. [https://doi.org/10.1175/1520-0426\(2003\)20<730:AAEAF>2.0.CO;2](https://doi.org/10.1175/1520-0426(2003)20<730:AAEAF>2.0.CO;2)
- Meehl, G. A., Arblaster, J. M., Fasullo, J. T., Hu, A., & Trenberth, K. E. (2011). Model-based evidence of deep-ocean heat uptake during surface-temperature hiatus periods. *Nature Climate Change*, *1*(7), 360–364. <https://doi.org/10.1038/nclimate1229>
- Moss, R. H., Edmonds, J. A., Hibbard, K. A., Manning, M. R., Rose, S. K., van Vuuren, D. P., et al. (2010). The next generation of scenarios for climate change research and assessment. *Nature*, *463*(7282), 747–756. <https://doi.org/10.1038/nature08823>
- Shields, C. A., Bailey, D. A., Danabasoglu, G., Kiehl, J. T., Levis, S., Jochum, M., & Park, S. (2012). The low-resolution CCSM4. *Journal of Climate*, *25*(12), 3993–4014. <https://doi.org/10.1175/JCLI-D-11-00260.1>

- Sriver, R. L., Forest, C. E., & Keller, K. (2015). Effects of initial conditions uncertainty on regional climate variability: An analysis using a low-resolution CESM ensemble. *Geophysical Research Letters*, *42*, 5468–5476. <https://doi.org/10.1002/2015GL064546>
- Trenberth, K. E., & Caron, J. M. (2001). Estimates of meridional atmosphere and ocean heat transports. *Journal of Climate*, *14*(16), 3433–3443. [https://doi.org/10.1175/1520-0442\(2001\)014<3433:EOMAAO>2.0.CO;2](https://doi.org/10.1175/1520-0442(2001)014<3433:EOMAAO>2.0.CO;2)
- Trenberth, K. E., & Fasullo, J. T. (2010). Tracking Earth's energy. *Science*, *328*(5976), 316–317. <https://doi.org/10.1126/science.1187272>
- Trenberth, K. E., Fasullo, J. T., & Kiehl, J. (2009). Earth's global energy budget. *Bulletin of the American Meteorological Society*, *90*(3), 311–324. <https://doi.org/10.1175/2008BAMS2634.1>
- Vega-Westhoff, B., & Sriver, R. L. (2017). Analysis of ENSO's response to unforced variability and anthropogenic forcing using CESM. *Scientific Reports*, *7*. <https://doi.org/10.1038/s4158-017-18459-8>
- Warren, B. A. (1983). Why is no deep water formed in the North Pacific? *Journal of Marine Research*, *41*(2), 327–347. <https://doi.org/10.1357/002224083788520207>
- Weaver, A. J., Bitz, C. M., Fanning, A. F., & Holland, M. M. (1999). Thermohaline circulation: High latitude phenomena and the difference between the Pacific and Atlantic. *Annual Review of Earth and Planetary Sciences*, *27*(1), 231–285. <https://doi.org/10.1146/annurev.earth.27.1.231>
- Yang, H., & Zhu, J. (2011). Equilibrium thermal response timescale of global oceans. *Geophysical Research Letters*, *38*, L14711. <https://doi.org/10.1029/2011GL048076>
- Zweng, M. M., Regan, J. R., Antonov, J. I., Locarnini, R. A., Mishonov, A. V., Boyer, T. P., et al. (2013). World ocean atlas 2013, volume 2. In S. Levitus & A. Mishonov (Eds.), *Salinity* (Vol. 74, p. 27). NOAA atlas NESDIS.